Comparison of Engineering Wake Models with CFD Simulations

2014 J. Phys.: Conf. Ser. 524 012161

(http://iopscience.iop.org/1742-6596/524/1/012161)

Comparison of Engineering Wake Models with CFD Simulations.

S. J. Andersen[1], J. N. Sørensen[1], S. Ivanell[2], R. F. Mikkelsen[1]

[1] Department of Wind Energy, Building 403,Technical University of Denmark, DK-2800 Lyngby, Denmark

[2] Wind Energy Campus Gotland, Dep. of Earth Sciences, Uppsala University, 621 67, Visby, Sweden.

E-mail: sjan@dtu.dk

Abstract. The engineering wake models by Jensen [1] and Frandsen et al. [2] are assessed for different scenarios simulated using Large Eddy Simulation and the Actuator Line method implemented in the Navier-Stokes equations. The scenarios include the far wake behind a single wind turbine, a long row of turbines in an atmospheric boundary layer, idealised cases of an infinitely long row of wind turbines and infinite wind farms with three different spacings. Both models include a wake expansion factor, which is calibrated to fit the simulated wake velocities. The analysis highlights physical deficiencies in the ability of the models to universally predict the wake velocities, as the expansion factor can be fitted for a given case, but with not apparent transition between the cases.

1. Introduction

Today, industry continues to employ a number of engineering wake models for assessing the velocity deficits and power production behind single and multiple wind turbines. Generally, these models are based on simple single wake calculations and steady state considerations. Furthermore, the models often assume self-similar velocity profiles in the far wake, which ensures simplicity and computational speed.

The models use different assumptions to superpose or account for merging wakes behind numerous wind turbines, which in turn is used to describe the overall wake interaction inside wind farms and the asymptotic equilibrium state of the 'infinite wind farm'. Notable models include the models by Jensen [1] and Frandsen et al. [2]. Jensen assumed the wake behind a wind turbine to be analogous to a negative jet with a linear wake expansion and derived an explicit expression for the asymptotic wind speed based on mass conservation. Frandsen et al. developed a wake model based on momentum analysis over a control volume for one or multiple turbines. Frandsen's solution assumes a linear expansion of the wake area. Frandsen's model for multiple turbines includes three distinct regimes, the first regime of multiple inline wake interaction, the second regime where the wake expansion is limited due to the ground and adjacent rows of turbines and their wake, and hence the combined wake can only expand vertically. Finally, the third regime models the equilibrium or infinite scenario, where the flow internally in the wind farm is in balance with the boundary layer created over the wind farm.

These engineering models are occasionally capable of giving good agreement, particular in terms of overall farm efficiency, although the results are generally not consistent. The models

still lack a thorough calibration and verification before they can be applied universally to all situations, particular inside large wind farms. Barthelmie et al. [3] compared six different wake models with measurements from Vindeby wind farm, which showed an average absolute error of 15% in determining the wind velocity at hub height and concluded: 'the spread of the wake model predictions is considerable even for these relative simple offshore single wake cases'.

Therefore, the present work sets out to compare such engineering wake models to Large Eddy Simulations employing the Actuator Line technique. A number of key features and assumptions of the wake models are investigated, i.e. the wake expansion and recovery behind a single turbine, the superposition assumption for a number of wind turbines as well as the asymptotic wind speed in the 'infinite wind farm'. The 'infinite wind farm' scenario has received increased attention as the size of wind farms continue to grow. Peña and Rathmann [4] investigated the effects of roughness and atmospheric stability for the infinite wind farm for the Park wake model (expanded Jensen wake model) and for the Frandsen model. Other recent work modelled the infinite wind farm using LES and investigated the effects of spacing, see Calaf et al. [5], Yang et al. [6], and Meyers and Meneveau [7]. The effects of thrust coefficient, turbine spacing, and vertical shear are investigated in the present work for the different scenarios. The original models by Jensen and Frandsen lump the majority of these effects into the same expansion factor, except the thrust coefficient, which is included either directly or through the induction factor. The aim is hence to assess and attempt to link the model performance in the different scenarios, and provide new calibrated parameters for the engineering models.

2. Methods

The expression derived in the engineering wake models by N. O. Jensen [1] and Frandsen et al. [2] are briefly described in the following as well as an outline of the flow solver and numerical simulations.

2.1. N. O. Jensen Model

N. O. Jensen makes an analogy between the wake deficit and a negative jet, which leads to the following expression for the velocity behind a single wind turbine:

$$\frac{U_J}{U_0} = 1 - 2 \cdot a \cdot \left(\frac{R}{R + \alpha_J \cdot X} \right)^2 \tag{1}$$

where R is the rotor radius, a is the induction factor, X the streamwise distance, and α_J is an entrainment or expansion constant, which governs the wake expansion. Jensen assumes an optimal rotor, i.e. $a = \frac{1}{3}$, but the more general expression is maintained here. Furthermore, the wake expansion is assumed linear, and Jensen originally suggested $\alpha_J = 0.10$, while more recent work, e.g. Barthelmie et al. [3], suggests $\alpha_J = 0.05$ for offshore wind turbines. The expansion constant is basically a calibration factor and of main interest in the current investigation.

Jensen extends the analysis to multiple(N) wind turbines. Assuming $a = \frac{1}{3}$ leads to the following explicit expression for the wake velocity:

$$u_{J,n} = \frac{U_J}{U_0} = 1 - 2 \cdot \frac{k}{3} \cdot \frac{1 - (\frac{k}{3})^n}{1 - \frac{k}{3}}, \qquad k = \left(\frac{R}{R + \alpha_{J,N} S} \right)^2 \tag{2}$$

where u_n is the wake velocity in front of the n'th turbine, S is the normalised turbine spacing in turbine radii, and $\alpha_{J,N}$ is the expansion factor for multiple turbine. Assuming $a = \frac{1}{3}$, means that a calibrated entrainment constant (through k) includes a correction for a non-optimal rotor.

As $k < 1$, the term $(\frac{k}{3})^n$ quickly vanishes for large N. Therefore, the asymptotic velocity or the velocity in an infinitely large wind farm is determined by:

$$u_{J,\infty} = 1 - \frac{2 \cdot \frac{k}{3}}{1 - \frac{k}{3}}, \qquad k = \left(\frac{R}{R + \alpha_{J,\infty} S}\right)^2 \tag{3}$$

where $\alpha_{J,\infty}$ is still the calibration constant.

2.2. Frandsen Model

Frandsen et al. [2] performs a control volume analysis and relates the wake velocity directly to the thrust coefficient. The expansion of the wake area is essentially a calibration parameter for a given C_T, see Frandsen et al. [2] for specific suggestions. Frandsen et al. suggest the following expression for the expansion of the wake diameter:

$$D(x) = \left(\beta^{\frac{k}{2}} + 2\alpha_F S\right)^{\frac{1}{k}} D_0, \qquad S = \frac{X}{R}, \qquad \beta = \frac{1}{2}\frac{1 + \sqrt{1 - C_T}}{\sqrt{1 - C_T}} \tag{4}$$

where β governs the initial expansion rate, so the basic assumption is that the wake expansion occurs immediately after the turbine as $A_a = \beta A_0$. α_F is an expansion constant similar to α_J, which needs to be determined experimentally. k is a shape factor which governs the order of the expansion and D_0 is the rotor diameter.

The wake velocity is determined as:

$$\frac{U_F}{U_0} = \frac{1}{2} \pm \frac{1}{2}\sqrt{1 - 2\frac{A_0}{A} C_T} \tag{5}$$

where $\frac{A_0}{A}$ gives the wake expansion in terms of the rotor area, A_0, and the wake area, A.

Similar to Jensen, Frandsen et al. also present an expression for the wake velocity in a long row of wind turbines and an asymptotic expression for the infinitely large wind farm. Frandsen et al. distinguish between three different regimes, but only the first regime is treated in the following. The wake velocity is determined from this recursive expression:

$$u_{F,n} = \frac{U_{F,n}}{U_0} = 1 - \left(\frac{A_{n-1}}{A_n} \cdot (1 - u_{F,n-1}) + \frac{1}{2}\frac{A_R}{A_n} C_T u_{F,n-1}\right) \tag{6}$$

where A_R is the rotor area and A_n the wake area for the n'th wake.

Finally, Frandsen's control volume analysis yields the following expression for the asymptotic relative velocity value:

$$u_{F,\infty} = \frac{U_F}{U_0} = \frac{\alpha_{F,\infty}}{\alpha_{F,\infty} + \frac{C_T}{S}} \tag{7}$$

where $\alpha_{F,\infty}$ is a constant governing the wake expansion in the asymptotic case. It is different from α_J, and as such subject to calibration. Frandsen et al. [2] and Barthelmie et al. [3] set $\alpha_F = \mathcal{O}(10 \cdot \alpha_J)$ for small C_T and large spacings. Note, that Frandsen et al. used the rotor diameter as reference, and it has been rewritten in terms of R for consistency.

Alternatively, if $\frac{U_F}{U_0}$ is known, then $\alpha_{F,\infty}$ can be determined from:

$$\alpha_{F,\infty} = \frac{C_T}{S}\frac{\frac{U_F}{U_0}}{1 - \frac{U_F}{U_0}} \tag{8}$$

2.3. Numerical Simulations

The numerical simulations are performed using the 3D flow solver EllipSys3D, which was developed as a collaboration between DTU(Michelsen [8]) and Risø(Sørensen[9]). EllipSys3D solves the discretised incompressible Navier-Stokes equations in general curvilinear coordinates using a block structured finite volume approach in primitive variables (pressure-velocity). The pressure correction equation is solved using the PISO algorithm and pressure decoupling is avoided using the Rhie-Chow interpolation technique. The convective terms are discretised through a hybrid scheme combining the third order accurate QUICK scheme and the fourth order CDS scheme. The hybrid scheme is employed as a compromise in order to avoid unphysical numerical wiggles, occurring when using a pure fourth order scheme, and at the same time limit numerical diffusion due to the upwind biasing nature of the QUICK scheme.

The influence of the wind turbine is simulated using the Actuator Line(AL) technique, see Sørensen and Shen [10] for full details on the AL technique. Body forces are distributed along rotating lines, which represents the wind turbine blades. The body forces used in the AL method are calculated using airfoil data and Flex5, a full aero-elastic code for calculating deflections and loads on wind turbines, see e.g. Øye [11]. The advantage of representing the individual blades by line-distributed forces is that much fewer grid points are needed to capture the influence of the blades, as compared to a fully resolved computation. Hence, the actuator line model enables a detailed study of the dynamics of the wake, as it includes the tip and root vortices, using a reasonably low number of grid points. The drawback of the method is that it relies on the quality of tabulated airfoil data. Airfoil data corresponding to the NM80 turbine is used in the present work. The 2D airfoil data is corrected to account for 3D effects. The NM80 is a three bladed wind turbine with a radius of $R = 40m$ and rated to $2.75MW$ at $V_{hub} = 14m/s$.

The wind turbine includes a controller, which is a combination of a variable speed P-controller for small wind speeds($V_{hub} < 14m/s$) and a PI-pitch angle controller for higher wind speeds, see e.g. Hansen et al. [12] for details of a comparable controller. The implemented controller essentially means that the rotor is not constantly loaded, and as such it operates like a real turbine as it responds to the incoming (turbulent) flow. Therefore, the flow solver and the aero-elastics are fully coupled through the employment of Flex5.

The flow field is thus simulated by solving the 3D incompressible Navier-Stokes equations:

$$\frac{\partial \overline{\mathbf{V}}}{\partial t} + \overline{\mathbf{V}} \cdot \nabla \overline{\mathbf{V}} = -\frac{1}{\rho}\nabla \overline{p} + \nabla[(\nu + \nu_{SGS})\nabla \overline{\mathbf{V}}] + \frac{1}{\rho}\mathbf{f}_{WT} + \frac{1}{\rho}\mathbf{f}_{turb} + \frac{1}{\rho}\mathbf{f}_{pbl} + \frac{1}{\rho}\mathbf{f}_{mf}. \tag{9}$$

$$\nabla \overline{\mathbf{V}} = 0. \tag{10}$$

where ρ denotes density, p is pressure, and ν is eddy viscosity. A number of actuators or body forces($\mathbf{f}_{WT}$, $\mathbf{f}_{turb}$, $\mathbf{f}_{pbl}$, and $\mathbf{f}_{mf}$) are explicitly applied in the simulations. These forces model the effect of the wind turbine, atmospheric turbulence, atmospheric boundary layer, and account for any loss in mass flux in the infinite cases. All the body forces are continuously updated to reach their objective except the forces for the atmospheric boundary layer. The forces for the prescribed atmospheric boundary layer is determined to fit a given vertical velocity profile through a precursor simulation and kept constant throughout the actual simulation. The desired velocity profile is given by:

$$U_{pbl}(z) = \begin{cases} U_0 \cdot (c_2 z^2 + c_1 z) & z \leq \Delta_{PBL} \\ U_0 \cdot \left(\frac{z}{H_{hub}}\right)^{\alpha_{PBL}} & z > \Delta_{PBL} \end{cases} \tag{11}$$

where $\Delta_{PBL} = 1R$ determines the height, where the profile shift from the parabolic to power law profile. $H_{hub} = 2R$ is the hub height, c_1, c_2, and α_{PBL} are shape parameters. c_1 and c_2 are

calculated to ensure a smooth transition between the parabolic and the power law expression using the following expressions:

$$c_1 = \frac{U_{hub}}{H_{hub}} \cdot (2 - \alpha_{PBL}) \cdot \left(\frac{\Delta_{PBL}}{H_{hub}}\right)^{(\alpha_{PBL}-1)} \tag{12}$$

$$c_2 = \frac{U_{hub}}{H_{hub}} \cdot \frac{1}{\Delta_{hub}} \cdot (\alpha_{PBL} - 1) \cdot \left(\frac{\Delta_{PBL}}{H_{hub}}\right)^{(\alpha_{PBL}-1)} \tag{13}$$

This approach to modelling the atmospheric boundary layer enables the use of any desired (e.g. measured) vertical velocity profile without a large precursor simulation for a numerically developing boundary layer, which requires calibration of surface roughness in the vicinity of the turbines and upstream. This method is independent of surface roughness, yet it provides the desired vertical velocity profile. The surface roughness elements would add some additional turbulence, but this is neglected based on the findings of Frandsen and Madsen [13], who investigated the influence of ambient turbulence in large wind farms and found the internal turbulence to be dominated by the inherent turbulence stemming from the turbines and the ambient atmospheric turbulence to be less relevant. Andersen [14] added additional atmospheric turbulence above the turbines, which only had a minor impact on the mixing and wake recovery in large wind farms.

The added turbulence is generated by the Mann model, see Mann [15] and [16] for details. The turbulent forces are imposed a few radii upstream the first turbine in the domain.

Additional details on the numerical implementation of the body forces can be found in Andersen [14].

2.4. Simulations Overview

Several simulations have been conducted to cover the different scenarios described by the engineering wake models and these will briefly be outlined in the following.

2.4.1. Single Turbine Two simulations have been conducted of the free wake development behind a single turbine, i.e. no atmospheric boundary layer and a minimum amount(0.1%) of added turbulence. The turbulence is added to break the numerical symmetry to initiate a more natural wake breakdown. The wake development is simulated up to $38R$ downstream. Far-field Dirichlet boundary conditions($U = constant$) are applied on the lateral and vertical boundary conditions. The two simulations differ in terms of tip-speed ratio and thrust coefficient, which are set to $\lambda = 7.78$ and $C_T = 0.75$ as well as $\lambda = 11.42$ and $C_T = 0.86$, respectively. The controller has not been applied for these simulations in order to keep a constant thrust and tip-speed ratio. More details about the simulations can be found in Kermani et al. [17].

2.4.2. Long Row of Turbines One simulation has been conducted for a long row of turbines, currently with 8 wind turbines. The turbine spacing is $S = 20R$ and the freestream velocity is $U_0 = 8m/s$. Far-field boundary conditions are applied on the top boundary with a slip boundary condition on the ground. This is chosen not to counteract the prescribed boundary layer, i.e. as there would otherwise develop a different boundary layer over time. Cyclic boundary conditions are applied in the lateral direction, but there is no interaction between the rows due to the large spacing. No atmospheric turbulence is introduced, but an atmospheric boundary layer is prescribed with $\alpha_{PBL} = 0.14$, see Equation 11. The first turbine in the row has a thrust coefficient of $C_T = 0.87$, which yields an induction factor of $a = 0.32 \approx \frac{1}{3}$.

2.4.3. Infinitely Long Row of Turbines and Infinite Wind Farm A total of six different simulations have been performed to simulate the infinite cases by applying cyclic boundary conditions in the flow direction. Three simulations are done without any atmospheric boundary layer to mimic an infinitely long row of turbines and three simulations include the effects of an atmospheric boundary layer as well as cyclic boundaries in the lateral direction to model an infinitely large wind farm. Far-field boundary conditions are applied on the lateral and vertical for the former as well as on the top boundary in the latter case. The latter case includes a slip boundary condition on the ground. The prescribed boundary layer for the latter cases is prescribed with $\alpha_{PBL} = 0.10$. The three simulations have different turbine spacings of $S = 12R$, $S = 16R$, and $S = 20R$ for both with and without the atmospheric boundary layer. The simulations have been run long enough for the statistical properties of the mean flow, turbulent intensities, Reynolds stresses, and Turbulent Kinetic Energy(TKE) production terms to converge. Further details of the convergence and the simulations in general can be found in Andersen [14].

3. Results

The engineering models have been fitted to the average, streamwise velocity at the center of the wake, i.e. at hub height. In the single turbine case, the velocity is extracted at various distances behind the turbine, while the reference velocity is taken as the velocity experienced by the wind turbine(s), when several turbines are modelled. This reference velocity is used by the controller and extracted from a reference point of $1R$ upstream the actual turbine plane. In the case of infinitely many wind turbines, the thrust coefficient is based on the same reference inflow velocity through:

$$C_T \approx \frac{7}{U_{hub}} \tag{14}$$

This relationship given by Frandsen [18] is adopted into the IEC standard [19] as a generic approximation for C_T, and it is a good approximation for the NM80 turbine, see Andersen [14].

3.1. Single Turbine

Jensen assumes a linear expansion of the wake, while Frandsen et al. suggests a wake expansion of $D \propto \sqrt{X}$, i.e. $k = 2$ which ensures a theoretical asymptotic flow speed for the infinite wind farm. The wake expansion has been assessed in two different ways. First method determines the wake radius(δ_1) as the point, where the average wake velocity($\overline{U}$) is half the wake center velocity(U_c)

$$\left.\frac{\overline{U}}{U_c}\right|_{\frac{\delta_1}{R}} = 0.5 \tag{15}$$

Second method determines the wake radius(δ_2), where the wake velocity($\overline{U}$) reach 99% of the freestream velocity(U_0)

$$\left.\frac{\overline{U}}{U_0}\right|_{\frac{\delta_2}{R}} < 0.99 \tag{16}$$

Figures 1 shows the wake expansion for both methods. It can be seen that the far wake region, where the models are valid, commence around $\frac{X}{R} > 12$, as the wake expansion is almost linear from this point onwards. Only the linear wake expansion in the far wake region is used for the subsequent fitting, and this region is marked by a thicker line. Clearly, the recommended values for Jensen and Frandsen do not yield good agreement with the actual expansion, except Jensen fits $\frac{\delta_2}{R}$ very well for $C_T = 0.86$. However, since the wake expansion is almost linear in the far wake, it is possible to determine the expansion factors which fit the far wake expansion in a least

squares sense. The induction factors and the fitted expansion factors are summarised in Table 1. It is clear that the fits for δ_2 are much better than those obtained for δ_1. The recommended value of $\alpha_J = 0.05$ for Jensen's linear wake expansion is a first good approximation, while Frandsen overestimates the expansion and the fitted factors are only $\mathcal{O}(4-6)\alpha_J$ and not $\mathcal{O}(10)\alpha_J$ as otherwise suggested by Frandsen et al. It has also been attempted to fit the combined effect of α and k for Frandsen, but it did not yield significant improvements.

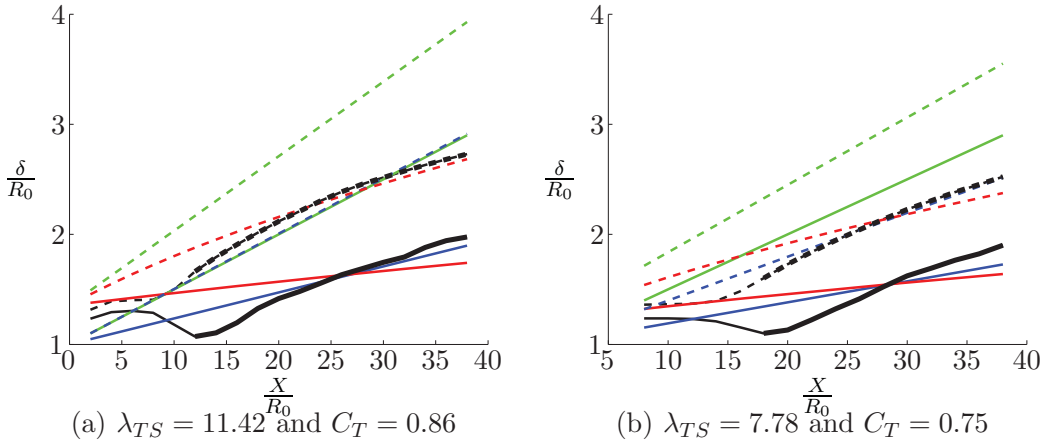

(a) $\lambda_{TS} = 11.42$ and $C_T = 0.86$ (b) $\lambda_{TS} = 7.78$ and $C_T = 0.75$

Figure 1. Wake expansion behind a single wind turbine. ——— : CFD, $\frac{\delta_1}{R}$. - - - : CFD, $\frac{\delta_2}{R}$. ——— : Jensen with $\alpha_J = 0.05$. - - - : Frandsen with $k = 2$, $\alpha = \beta^{k/2}[(1+2\alpha_J s)^k - 1]s^{-1}$ and $\beta = \frac{1}{2}\frac{1+\sqrt{1-CT}}{\sqrt{1-CT}}$. ——— : Jensen fit to $\frac{\delta_1}{R}$. - - - : Jensen fit to $\frac{\delta_2}{R}$. ——— : Frandsen fit to $\frac{\delta_1}{R}$. - - - : Frandsen fit to $\frac{\delta_2}{R}$.

Table 1. Wake expansion factors behind a single wind turbine and the corresponding coefficient of determination(R^2) computed between the models and LES data. Subscript J refer to the model by Jensen, while F refer to the model by Frandsen et al.

$\lambda_{TS} = 11.42$ and $C_T = 0.86$	$\lambda_{TS} = 7.78$ and $C_T = 0.75$
$a = 0.3129$	$a = 0.2500$
$\alpha_{J,\delta_1} = 0.0236$ $\alpha_{J,\delta_2} = 0.0504$	$\alpha_{J,\delta_1} = 0.0191$ $\alpha_{J,\delta_2} = 0.0399$
$\alpha_{F,\delta_1} = 0.0629$ $\alpha_{F,\delta_2} = 0.2823$	$\alpha_{F,\delta_1} = 0.0629$ $\alpha_{F,\delta_2} = 0.2179$

Figures 2 shows the computed center velocities based on the different expansion factors. The unfitted expressions using recommended values overestimates the velocities, although Jensen gives a better agreement than Frandsen for both cases. Fitting to δ_1 yields an underestimate of the velocities, while fitting to δ_2 yields a minor improvement compared to the recommended values for both engineering models. Generally, Jensen gives better results. The best fits overestimates the velocities by more than 20% in the initial far wake($12R - 20R$), while it

only overestimates by $2-3\%$ for the very far wake($25R+$). The models could naturally be fitted to a more limited range instead of the entire far wake region of $12R-38R$. However, it highlights a physical deficiency, and hence limitations, of the model's capability to predict the correct wake development even in the far wake, where the models should be valid. It also shows that the far wake might be reached further downstream than usually assumed.

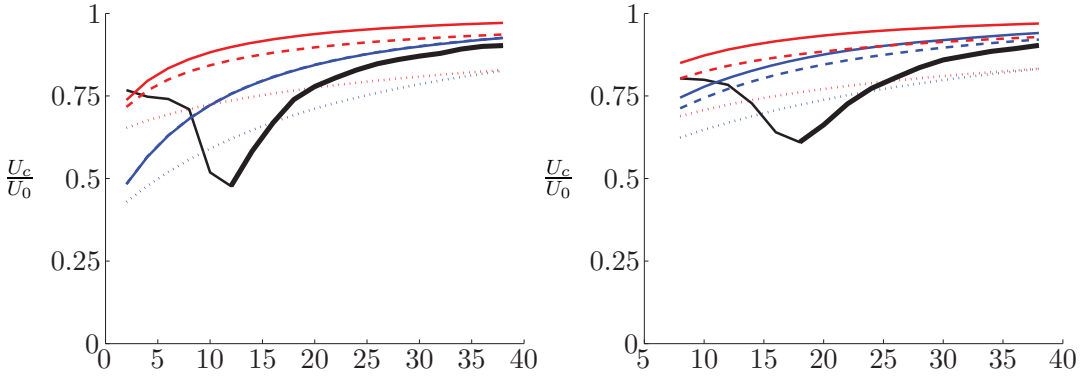

(a) $\lambda_{TS} = 11.42$ and $C_T = 0.86$ (b) $\lambda_{TS} = 7.78$ and $C_T = 0.75$

Figure 2. Center wake velocity behind a single wind turbine. ——— : CFD, U_c. ——— : Jensen with $\alpha_J = 0.05$. - - - : Jensen fit to $\frac{\delta_1}{R}$. ····· : Jensen fit to $\frac{\delta_2}{R}$. ——— : Frandsen with $\alpha_J = 0.05$. - - - : Frandsen fit to $\frac{\delta_1}{R}$. ····· : Frandsen fit to $\frac{\delta_2}{R}$.

3.2. Long Row of Turbines

The wake prediction is of particular of interest when one or more turbines are aligned. The Jensen model is fitted directly to the wake velocity in the long row of wind turbines, see Equation 2. Frandsens model is basically fitted through the expression for the wake expansion. The wake expansion from the CFD results are hence assessed by matching the wake velocities to Equation 6. Subsequently, the expression for the wake expansion(Equation 4) is fitted to these assessed wake areas. Figure 3 shows the assessed and fitted wake expansions. Frandsen et al. derives an expression for the wake expansion, which includes an initial and immediate wake expansion behind the first turbine of $A_a = \beta A_0$, but comments that neglecting the initial wake expansion has proven successful, when employing WAsP [20]. That is also the case here. Neglecting the initial wake expansion and fitting to the assessed wake expansion yields a very good and linear agreement. The wake expansion is also shown as a radial expansion($\delta = \sqrt{\frac{A}{\pi}}$), although a circular wake is not a precondition of the Frandsen model. This validates that the turbines are still operating within the 1st regime as $\frac{\delta}{R} \leq 2$, hence Equation 6 is still valid. The only outlying point is the assessed wake expansion at the second turbine. The discrepancy is caused by the relative low velocity of only $0.55U_0$, which recovers to $0.65U_0$ for the third turbine.

The velocity and the fitted velocities using Jensen and Frandsen et al. are also shown in Figure 3. The overall agreement is very good from the third to the eighth turbine. Jensen predicts a maximum discrepancy of 4.2%, while Frandsen yields differences of up to 9.7%. The turbulence introduced by the first and second turbine effectively aids in the wake recovery, which results in the higher velocity experienced by the third and following turbines.

The fitted parameters are $\alpha_{J,N} = 0.0258$ and $\alpha_{F,N} = 0.0189$ for a row of eight turbines. These parameters are similar to the fitted parameters for the far wake behind a single turbine, which could indicate a direct transition between the two scenarios.

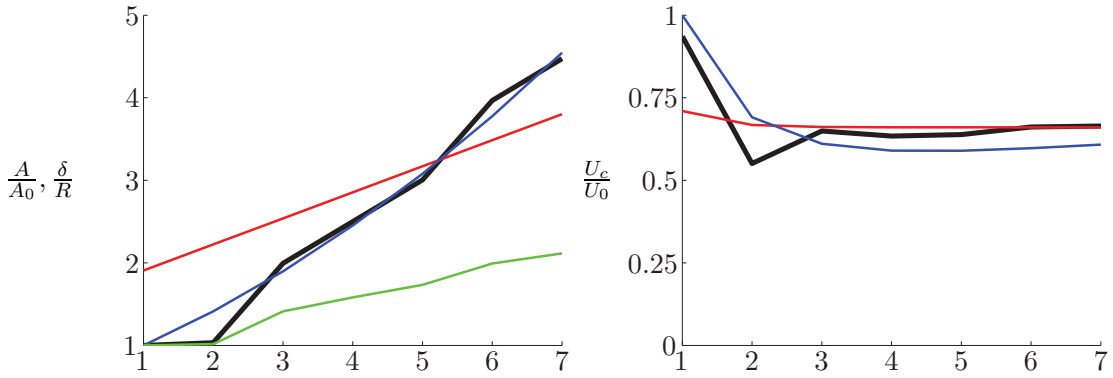

(a) Assessed wake expansion. (b) Center wake velocity.

Figure 3. Fitted wake expansion and wake velocity in a long row of wind turbines. Figure a): ▬ : Assessed areal wake expansion from CFD. ▬ : Frandsen including initial wake expansion, $A_a = \beta A_0$. ▬ : Frandsen excluding initial wake expansion. ▬ : Assessed radial wake expansion from CFD, $\frac{\delta}{R}$. Figure b): ▬ : Center wake velocity from CFD. ▬ : Jensen fit. ▬ : Frandsen fit excluding initial wake expansion.

3.3. Infinitely Long Row of Turbines

Figure 3 clearly indicates how the internal wind speed deep inside a large array of wind turbines tends towards an asymptotic value. Jensen and Frandsen et al. both gave expressions for this infinite wake case. Equations 3 and 8 are used to determine $\alpha_{J,\infty}$ and $\alpha_{F,\infty}$.

Two cases have been considered. An infinite row of turbines and an infinitely large wind farms in a atmospheric boundary layer. The fitted wake expansion factors for the infinite row of turbines are given in Table 2 as well as the asymptotic velocity and thrust coefficients based on Equation 14. The wake velocity is clearly increased as the turbine spacing increases, although there are no large differences for the three spacings. There is a decreasing trend for the expansion factor for increasing turbine spacing for both engineering models.

Table 2. Wake expansion factors for infinite row of turbines.

$S = 12R$	$S = 16R$	$S = 20R$
$\frac{\overline{U_c}}{U_0} = 0.74$	$\frac{\overline{U_c}}{U_0} = 0.76$	$\frac{\overline{U_c}}{U_0} = 0.78$
$C_T = 0.63$	$C_T = 0.61$	$C_T = 0.60$
$\alpha_{J,\infty} = 2.34$	$\alpha_{J,\infty} = 1.91$	$\alpha_{J,\infty} = 1.67$
$\alpha_{F,\infty} = 0.15$	$\alpha_{F,\infty} = 0.12$	$\alpha_{F,\infty} = 0.11$

Similarly, Table 3 gives the asymptotic wake velocity, thrust coefficient, and fitted expansion factors for the infinite wind farm with an atmospheric boundary layer. The velocities have once again been fitted to Equations 3 and 8. The effect of the boundary layer clearly decrease the velocity for small spacings, while it increase the recovery for larger spacings compared to the infinitely long row of turbines. As opposed to the previous case with no atmospheric boundary layer, the expansion factors now increase with increasing turbine spacing.

Table 3. Wake expansion factors for infinite wind farm with ABL.

$S = 12R$	$S = 16R$	$S = 20R$
$\frac{\overline{U_c}}{U_0} = 0.61$	$\frac{\overline{U_c}}{U_0} = 0.73$	$\frac{\overline{U_c}}{U_0} = 0.80$
$C_T = 0.77$	$C_T = 0.64$	$C_T = 0.58$
$\alpha_{J,\infty} = 1.43$	$\alpha_{J,\infty} = 1.69$	$\alpha_{J,\infty} = 1.83$
$\alpha_{F,\infty} = 0.10$	$\alpha_{F,\infty} = 0.11$	$\alpha_{F,\infty} = 0.12$

It is noteworthy, how the expansion factors for both infinite cases are significantly larger than the corresponding expansion factors from the previous cases. $\alpha_{J,\infty}$ is $\mathcal{O}(75-100)$ larger, while $\alpha_{F,\infty}$ is $\mathcal{O}(5)$ larger than the previous parameters. This indicates that as the infinite cases are achieved, the entrainment takes over the effect of the wake expansion in the expansion factor as it accounts for the increased wake recovery through turbulent mixing in order to achieve the asymptotic state.

4. Discussion and Conclusion

A number of numerical simulations have been performed using EllipSys3D to model various wake scenarios behind a single, multiple, and infinitely many wind turbines. The numerical results are used to assess and calibrate two engineering wake models. Both models include a calibration parameter, which is related to the wake expansion. The wake expansion factor is shown to depend on thrust coefficient in the case of single wind turbine. Expansion factors in the same order of magnitude are found for a long row of (eight) wind turbines with an atmospheric boundary layer. The calibrated expansion factors for these scenarios are found to be approximately half of the recommended standard values. The calibrated expansion factors depends on the turbine spacing for the infinite cases, but is negatively correlated for the infinite row with no boundary layer and positively correlated for the infinite wind farm in a boundary layer, albeit in the same order of magnitude. The expansion factors are significantly larger for the final cases of an infinite row of turbines and infinitely large wind farms with atmospheric boundary layer, which accentuate the inability to bridge the different scenarios through a common expansion factor.

5. Acknowledgements

The present work has been carried out with the support of Vattenfall, the Danish Council for Strategic Research for the project 'Center for Computational Wind Turbine Aerodynamics and Atmospheric Turbulence'(COMWIND) (grant 2104-09-067216/DSF), and the Nordic Consortium on Optimization and Control of Wind Farms, which has provided valuable access to the National Supercomputer Centre in Sweden(NSC). Finally, the proprietary data for Vestas' NM80 turbine has been used.

References

[1] Jensen N O 1983 A note on wind generator interaction
[2] Frandsen S, Barthelmie R, Pryor S, Rathmann O, Larsen S, Højstrup J and Thøgersen M 2006 *Wind Energy* **9** 39–53
[3] Barthelmie R, Folkerts L, Larsen G, Rados K, Pryor S, Frandsen S, Lange B and Schepers G 2006 *J. Atmos. Ocean. Technol.* **23** 888–901
[4] Peña A and Rathmann O 2013 *Wind Energy* ISSN 1099-1824 URL `http://dx.doi.org/10.1002/we.1632`
[5] Calaf M, Meneceau C and Meyers J 2010 *Phys. Fluids* **22**

[6] Yang X, Kang S and Sotiropoulos F 2012 *Physics of Fluids (1994-present)* **24**
[7] Meyers J and Meneveau C 2012 *Wind Energy* **15** 305–317 ISSN 1099-1824 URL `http://dx.doi.org/10.1002/we.469`
[8] Michelsen J A 1992 *Report AFM*
[9] Sørensen N N 1995 *General Purpose Flow Solver Applied to Flow over Hills* Ph.D. thesis Technical University of Denmark
[10] Sørensen J N and Shen W Z 2002 *Journal of Fluids Engineering* **124** 393–399
[11] Øye S 1996 Flex4 simulation of wind turbine dynamics
[12] Hansen M H, Hansen A, Larsen T J, Oye S, Sorensen P and Fuglsang P 2005 *Control design for a pitch-regulated, variable speed wind turbine* Denmark. Forskningscenter Risœ. Risœ-R (Danmarks Tekniske Universitet, Risø Nationallaboratoriet for Bæredygtig Energi)
[13] Frandsen S and Madsen P 2003 *Spatially average of turbulence intensity inside large wind turbine arrays* (Univ. of Naples) pp 97–106
[14] Andersen S J 2013 *Simulation and Prediction of Wakes and Wake Interaction in Wind Farms* Ph.D. thesis Technical University of Denmark, Wind Energy.
[15] Mann J 1994 *Journal of Fluid Mechanics* **273** 141–168 ISSN 1469-7645
[16] Mann J 1998 *Probabilistic Engineering Mechanics* **13** 269–282 ISSN 0266-8920
[17] Kermani N A, Andersen S J, Sørensen J N and Shen W Z 2013 *Proceedings of 2013 International Conference on Aerodynamics of Offshore Wind Energy Systems and Wakes (ICOWES2013).*
[18] Frandsen S 2007 *Turbulence and turbulence-generated structural loading in wind turbine clusters* Denmark. Forskningscenter Risoe. Risoe-R ISBN 87-550-3458-6 risø-R-1188(EN)
[19] Amendment 1 to IEC 61400-1 Ed 3 2009 Wind turbines - part 1: Design requirements.
[20] Troen I and Petersen E L 1989 *European Wind Atlas* (Danmarks Tekniske Universitet, Risø Nationallaboratoriet for Bæredygtig Energi) ISBN 87-550-1482-8